Anomalous Moisture Diffusion in an Epoxy Adhesive Detected by Magnetic Resonance Imaging

Gabriel LaPlante,[1] Alexei V. Ouriadov,[2] Pearl Lee-Sullivan,[3] Bruce J. Balcom[4]

[1]*Department of Mechanical Engineering, Université de Moncton, Moncton, New Brunswick, Canada E1A 3E9*
[2]*Imaging Research Laboratories, Robarts Research Institute, University of Western Ontario, P. O. Box 5015, London, Ontario, Canada N6A 5K8*
[3]*Department of Mechanical and Mechatronics Engineering, University of Waterloo, 200 University Avenue West, Waterloo, Ontario, Canada N2L 3G1*
[4]*MRI Centre, Department of Physics, University of New Brunswick, P. O. Box 4400, Fredericton, New Brunswick, Canada E3B 5A3*

Received 1 October 2007; accepted 19 January 2008
DOI 10.1002/app.28106
Published online 17 April 2008 in Wiley InterScience (www.interscience.wiley.com).

ABSTRACT: Non-Fickian or anomalous diffusion is frequently observed when the absorption of moisture by a polymer is being studied. Different models have been presented in the literature that can accurately predict the trends of the weight-gain curves. However, it is not always clear which of these models yield good predictions of moisture distribution. This article presents a time-resolved moisture distribution study of an epoxy sample immersed in deuterated water (D_2O) at 70°C over a period of 2.5 months. The moisture distribution was measured during that period with a novel high-resolution magnetic resonance imaging technique that is well adapted to the imaging of thin plates. The experimental results showed that the concentration of D_2O at the surface of the sample increased with time, even after 2.5 months. These results were used to evaluate the performance of several standard diffusion models. Although this study is phenomenological, it appears that a model featuring time-varying boundary conditions yields the best representation of moisture absorption for these samples. © 2008 Wiley Periodicals, Inc. J Appl Polym Sci 109: 1350–1359, 2008

Key words: adhesives; diffusion; NMR

INTRODUCTION

Polymeric materials are being increasingly employed for advanced structural applications in many industries. The aerospace industry, in particular, is making increasing use of polymeric materials in the new generation of civil aircraft. Polymer matrix composites are expected to account for 16% of the weight of the new Airbus A380-800 airframe. The most widely used matrices in fiber-reinforced composites are epoxy-based. Epoxies are also used as adhesives for bonding joints and multilayered sandwich panels. Epoxies are employed mainly because of their superior chemical resistance and ease of manufacturing (e.g., low viscosity before cure and low cure shrinkage). It is recognized, however, that the mechanical properties of epoxy are influenced by the presence of moisture, even in small quantities of the order of 5 wt % or less.[1] Moisture in the environment is absorbed by epoxy and contributes to the loss of mechanical properties.[2] Recently, adhesive degradation due to moisture was found to be responsible for some structural problems with military aircraft.[3]

The mechanisms of moisture absorption by polymeric materials have been the subject of numerous studies.[4] Reviews by Apicella and Nicolais[5] and Weitsman[4,6] suggest that the sorption dynamics are very complex and depend on the polymer type, its history, and the conditions under which the experiments are performed.

Numerous models[7–10] of moisture absorption in polymers have been developed over the years that are based on observed phenomena and intuition. The simplest models are based on Fick's law. Simple Fickian diffusion models assume that there are no interactions between the sorbed water molecules and the polymer chains. Frequently, the Fickian models do not adequately represent the absorption process. Such cases are called non-Fickian or anomalous diffusion. Several different models have been proposed

Correspondence to: G. LaPlante (gabriel.laplante@umoncton.ca).

Contract grant sponsors: Natural Sciences and Engineering Research Council of Canada (to B.J.B. and P.L.-S. and for support of the University of New Brunswick Magnetic Resonance Imaging Centre by a Natural Sciences and Engineering Research Council of Canada Major Facilities Access grant), Canadian Department of National Defence, Defense Research and Development Canada (to B.J.B. and P.L.-S.).

to predict the moisture distribution and the total moisture uptake in a polymer during a non-Fickian absorption process. Carter and Kibler[8] showed that a two-phase Langmuir model could accurately reproduce moisture-uptake curves. The Langmuir model includes water molecule/polymer interactions by assuming that water molecules can exist in one of two states, free or bound, and that there is a dynamic exchange process between the two states. Maggana and Pissis[11] showed that anomalous diffusion could result from the combination of two independent Fickian processes characterized by a higher diffusion coefficient associated with free water diffusing in low-crosslink-density regions and a lower diffusion coefficient associated with water diffusing through high-crosslink-density regions. Crank[7] suggested that anomalous diffusion could be due to viscoelastic relaxation mechanisms in the polymer. Weitsman[6] showed that anomalous absorption can be explained by changing boundary conditions due to viscoelasticity. Roy et al.[10] proposed a model in which viscoelasticity is reflected as a change in the diffusion coefficient with time.

The vast majority of the diffusion model results presented in the literature are based on water uptake measurements. Although such measurements are very useful, they do not reveal any information about the spatial and temporal distribution of moisture within the polymer. Weitsman[4,6] pointed out the scarcity of moisture distribution data. Traditional methods used to obtain moisture profiles are frequently destructive[1] and therefore not well adapted to time-resolved studies.

In this article, a novel magnetic resonance imaging (MRI) technique was used to track the absorption of moisture by epoxy over an extended period of time. MRI has already been used by researchers to observe water penetration in polymers.[12] This method offers many advantages. It is nondestructive, therefore allowing the use of a single specimen during a time-resolved study. It is accurate and rapid enough that a measurement can be taken on a sample without significantly disturbing the absorption process. In this study, MRI was employed to obtain accurate moisture distribution profiles in a thin plate during the absorption process. The results provide insight into the absorption of moisture by an epoxy. Several moisture-absorption models are evaluated on the basis of the measured water distribution.

THEORY

This section presents the governing equations and the corresponding solutions for four of the most widely accepted models for moisture absorption by polymers. The Fickian model is the most basic diffusion model. The time-varying diffusivity and time-varying boundary condition models incorporate modifications to the Fickian model to account for viscoelasticity effects. The Langmuir model differs from the Fickian model through the inclusion of molecular interactions between the diffusing and absorbing media. Based on contemporary knowledge of diffusion in polymers,[4] all of these models possess some real characteristics of moisture absorption in polymers.

Fickian model

The simplest diffusion model is based on Fick's second law. For one-dimensional diffusion, the corresponding governing equation is

$$\frac{\partial c}{\partial t} = D\frac{\partial^2 c}{\partial x^2} \tag{1}$$

where c is the moisture concentration, D is the diffusion coefficient, t is the time, and x is the spatial coordinate. For the case of a thin plate of thickness $2h$ that has its surfaces suddenly exposed to a constant moisture concentration [the moisture concentration at the boundary (c_0)], the boundary conditions of eq. (1) are expressed as follows:

$$c(\pm h) = 0, \;\; t < 0 \qquad c(\pm h) = c_0, \;\; t \geq 0 \tag{2}$$

For a plate that is initially dry, the analytical solution to eqs. (1) and (2) is given by[7]

$$\frac{c(x,t)}{c_0} = 1 - \frac{4}{\pi}\sum_{n=0}^{\infty}\frac{(-1)^n}{2n+1}\exp\left[-\frac{D(2n+1)^2\pi^2 t}{4h^2}\right] \times \cos\frac{(2n+1)\pi x}{2h} \tag{3}$$

Two parameters govern Fickian diffusion: D and c_0. In practice, the values of these parameters are determined from the moisture-absorption curve. An analytical solution for the total moisture [m(+)] uptake is given by[7]

$$\frac{M(t)}{M_\infty} = 1 - \frac{8}{\pi^2}\sum_{n=0}^{\infty}\frac{1}{(2n+1)^2}\exp\left[-\frac{D(2n+1)^2\pi^2 t}{4h^2}\right] \tag{4}$$

where M_∞ is the amount of moisture absorbed at saturation.

A useful approximate closed-form solution for eq. (4) is given by[13]

$$\frac{M(t)}{M_\infty} = 1 - \exp\left[-7.3\left(\frac{Dt}{4h^2}\right)^{0.75}\right] \tag{5}$$

Fitting eqs. (4) or (5) to experimental data points yields D and c_0 ($c_0 = M_\infty/2h$). Alternatively, D can

be obtained from the initial slope of the moisture absorption curve as[13]

$$D = \pi\left(\frac{2h}{4M_\infty}\right)^2\left(\frac{M_2 - M_1}{\sqrt{t_2} - \sqrt{t_1}}\right)^2 \quad (6)$$

where subscripts 1 and 2 refer to two points located in the initial (linear) portion of the absorption curve.

Time-varying diffusion coefficient

Roy et al.[10] proposed that the effects of viscoelasticity on the absorption of moisture by polymers could be accounted for by the inclusion of a time-dependent diffusion coefficient in the governing equation. They showed that moisture absorption can be represented by the modification of eq. (1) to include a diffusion coefficient that increases exponentially to a plateau in the form of a Prony series. In this case, the diffusion coefficient in eq. (1) takes the following form:

$$D(t) = D_i + \sum_r D_r[1 - \exp(-t/\tau_r)] \quad (7)$$

where D_i and D_r are prony coefficients and τ_r is the rth time constant governing the time variation of D.

The analytical solution for this case is given by[10]

$$\frac{c(x,t)}{c_0} = 1 - \frac{4}{\pi}\sum_{n=0}^{\infty}\frac{(-1)^n}{2n+1}\exp\left\{\frac{-(2n+1)^2\pi^2}{4h^2} \times\left[D_i t + \sum_{r=1}^{R} D_r[t + \tau_r(e^{-t/\tau_r} - 1)]\right]\right\}\cos\frac{(2n+1)\pi x}{2h} \quad (8)$$

The corresponding moisture-uptake curve is given by

$$\frac{M(t)}{M_\infty} = 1 - \frac{8}{\pi^2}\sum_{n=0}^{\infty}\frac{1}{(2n+1)^2}\exp\left\{\frac{-(2n+1)^2\pi^2}{4h^2} \times\left\{D_i t + \sum_{r=1}^{R} D_r[t + \tau_r(e^{-t/\tau_r} - 1)]\right\}\right\} \quad (9)$$

The governing parameters M_∞, D_i, D_r, and τ_r are obtained by the fitting of eq. (9) to experimental absorption data.

Time-varying boundary conditions

Time-dependent boundary conditions were proposed by Weitsman[4] to model the absorption of moisture by polymers in which viscoelasticity causes the value of the moisture concentration at the exposed surfaces to increase with time. Cai and Weitsman[9] showed that moisture absorption in polymers could be modeled by allowing the surface concentrations to rise exponentially to a plateau. The boundary conditions in this case take the form of a Prony series:

$$c_0(t) = c_i + \sum_r c_r[1 - \exp(-t/\tau_r)] \quad (10)$$

where c_i and c_r are prony coefficients and τ_r is the rth time constant governing the time variation in the surface concentration. Crank[7] presented a solution for the case in which c_i is 0 and the change in c_0 can be described by one single-exponential term. The solution is

$$\frac{c(x,t)}{c_\infty} = 1 - \exp(-\beta t)\frac{\cos[x(\beta/D)^{0.5}]}{\cos[h(\beta/D)^{0.5}]} - \frac{16\beta h^2}{\pi}\sum_{n=0}^{\infty}\frac{(-1)^n}{2n+1}\frac{\exp[-D(2n+1)^2\pi^2 t/4h^2]}{[4\beta h^2 - D\pi^2(2n+1)^2]} \times\cos\frac{(2n+1)\pi x}{2h} \quad (11)$$

where c_∞ is the surface concentration at saturation and $\beta = 1/\tau$.

The moisture-uptake curve in this case is

$$\frac{M(t)}{M_\infty} = 1 - [\exp(-\beta t)](D/\beta h^2)^{0.5}\tan(\beta h^2/D)^{0.5} - \frac{8}{\pi^2}\sum_{n=0}^{\infty}\frac{1}{(2n+1)^2}\frac{\exp[-D(2n+1)^2\pi^2 t/(4h^2)]}{1 - (2n+1)^2[D\pi^2/(4\beta h^2)]} \quad (12)$$

In the general case in which the surface moisture concentration is represented by eq. (10), the moisture distribution is given by a linear combination of eqs. (3) and (11):[9]

$$\frac{c(x,t)}{c_\infty} = \frac{c_i c_H(x,t)}{c_\infty} + \sum_{r=1}^{R}\frac{c_r}{c_\infty}\hat{c}(x,t;\beta_r) \quad (13)$$

where c_H is Fick's solution [eq. (3)] and $\hat{c}$ is the solution for a surface concentration governed by a single-exponential rise [eq. (11)]. The corresponding moisture absorption is

$$\frac{M(t)}{M_\infty} = \frac{c_i}{c_\infty}M_H(t) + \sum_{r=1}^{R}\frac{c_r}{c_\infty}\hat{M}(t;\beta_r) \quad (14)$$

where M_H and $\hat{M}$ are the moisture uptakes [M(t)] given by eqs. (4) and (12), respectively and β_r is $1/\tau_r$.

The governing parameters c_∞ ($M_\infty/2h$), c_i, c_r, and β_r are obtained by the fitting of eq. (14) to the experimental absorption data.

Langmuir model

The aforementioned models assume that there are no chemical interactions between sorbed water mole-

cules and reactive sites in the epoxy; that is, all water molecules are diffusing freely. This assumption is not valid when the diffusing water forms bonds with reactive groups present in the epoxy, which affect the diffusion characteristics. The Langmuir two-phase model accounts for such interactions by assuming that the water molecules exist in two different states: free and bound. The one-dimensional governing equations in this case are[8]

$$D\frac{\partial^2 c_f}{\partial x^2} = \frac{\partial c_f}{\partial t} + \frac{\partial c_b}{\partial t}$$
$$\frac{\partial c_b}{\partial t} = \gamma c_f - \beta c_b \tag{15}$$

where subscript f and b refer to free and bound water, respectively. Parameters γ and β are the probabilities of free molecules becoming bound and bound molecules becoming free. At equilibrium, that is, saturation, $\gamma c_{f\infty} = \beta c_{b\infty}$.

The free water distribution given by the Langmuir model is[8]

$$\frac{c_f(x,t)}{x_{f_\infty}} = 1 - \frac{4}{\pi}\sum_{n=1}^{\infty(\text{odd})}\frac{(-1)^{n-1/2}}{n(r_n^+ - r_n^-)}\left[r_n^+\exp(-r_n^- t) - r_n^-\exp(r_n^+ t)\right]\cos\frac{\pi n x}{2h} + \frac{4}{\pi\beta}\sum_{n=1}^{\infty(\text{odd})}\frac{(-1)^{(n-1)/2}}{n(r_n^+ - r_n^-)}r_n^+ r_n^- \times\left[\exp(-r_n^- t) - \exp(-r_n^+ t)\right]\cos\frac{\pi n x}{2h} \tag{16}$$

where

$$r_n^\pm = \frac{1}{2}\left\{\kappa n^2 + \gamma + \beta \pm \left[(\kappa n^2 + \gamma + \beta)^2 - 4\kappa\beta n^2\right]^{0.5}\right\} \tag{17}$$

and

$$\kappa = \frac{\pi^2 D}{4h^2} \tag{18}$$

The total moisture uptake in this case is approximated by

$$\frac{M(t)}{M_\infty} \approx \frac{\beta}{\gamma+\beta}\exp(-\gamma t)\left[1 - \exp\left(-7.3\left(\frac{Dt}{4h^2}\right)^{0.75}\right)\right] + \frac{\beta}{\gamma+\beta}\left[\exp(-\beta t) - \exp(-\gamma t)\right] + \left[1 - \exp(-\beta t)\right] \tag{19}$$

for $2\gamma, 2\beta < \pi^2 D/(4h^2)$. The process is governed by parameters γ, β, M_∞, and D, which are obtained by the fitting of eq. (19) to moisture-uptake data.

EXPERIMENTAL

Specimen preparation

The epoxy used in this study was Cytec FM300 (Cytec Engineered Materials, Havre de Grace, MD), a high-temperature epoxy widely used in the aerospace industry. Thin sheets of epoxy were stacked to fabricate a plate of a nominal thickness of 1.5 mm. The plate was cured at a high temperature (177°C) *in vacuo* for 1 h according to the manufacturer's recommendations. Differential scanning calorimetry tests performed on small samples from the plate showed that the adhesive was fully cured. A full description of the specimen preparation is given elsewhere.[2]

One sample (30 mm × 35 mm) was cut from the plate for this MRI investigation. The thickness of the sample, measured with a micrometer, varied from 1.495 to 1.614 mm and was assumed to be uniform for the purpose of this study. The aspect ratio of the sample ensured that effects of absorption from the edges were negligible. The sample in its dry state was carefully weighed on an electronic balance with a precision of ±0.0001 g. It was then fully immersed in a reservoir containing deuterated water (D_2O) preheated to 70°C. The reservoir was loosely sealed and placed in an oven with the temperature controlled at 70°C. This procedure prevented pressure buildup inside the reservoir yet minimized D_2O loss due to evaporation. The temperature of immersion (70°C) was chosen carefully to maximize the diffusion rate without causing polymeric chain damage, as suggested by ASTM D 5229.[14] Intermittently, the sample was taken out of the reservoir, wiped dry with a lint-free cloth, and weighed. The mass data were used to construct the water uptake curve.

MRI

Nuclear magnetic resonance (NMR) is a phenomenon by which certain nuclei, in the presence of a magnetic field, oscillate at a frequency that depends on the magnetic field strength and on the nature of the nuclei. MRI is a well-known technique in clinical radiology but has also been proven to be well suited, with appropriate methodologies, for material science applications.[15]

MRI is a form of radio-frequency spectroscopy in which the magnetic resonance signal is encoded with position information to create noninvasive one-, two-, or three-dimensional images of objects. In this study, D_2O was selected over regular water (H_2O) as the diffusing fluid. This is because hydrogen (^1H) is present in significant quantities in the epoxy formulation. As a result, the ^1H signal from the polymer dominates the NMR signal as determined in preliminary measurements. The natural abundance of ^2H, on the other hand, is estimated to be approximately 0.015%. Therefore, the ^2H signal obtained from the

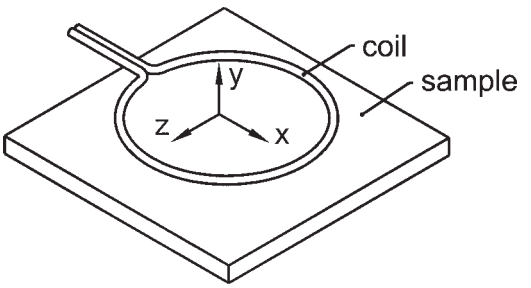

Figure 1 Schematic of the MRI measurement with a surface coil probe. The coil diameter is 25 mm. The surface coil area defines the region of interest in the MRI measurement. The nominal sample thickness is 1.6 mm. The y axis is the imaging axis.

conditioned sample will correspond exclusively to sorbed water. Deuterium (^{2}H) has a gyromagnetic ratio (γ) of 6.5×10^6 Hz/T, which is $\sim 1/6$ of γ for ^{1}H (4.26×10^7 Hz/T).

The one-dimensional nature of the diffusion process in a thin plate lends itself to MRI with a surface coil excitation method.[16] A local surface coil probe will limit the measurement to a small region of the sample. This constitutes an advantage when edge effects are to be avoided. A purpose-built surface coil probe with a diameter of 25 mm was used for this study. The probe configuration is depicted in Figure 1.

The selection of the MRI pulse sequence was dictated by the problem. A high resolution was desired for moisture profiles, and the sample had relatively short spin-spin relaxation time (T_2) and spin-spin relaxation time in an inhomogeneous magnetic field (T_2*) signal lifetimes (1–2 ms). This suggested the use of a phase encoding method. In addition, because of the weakness of the D_2O signal, high sensitivity was important. The selected method was the spin-echo single-point imaging method presented by Ouriadov et al.[16] This MRI method is well suited to the study of thin-film specimens measured with surface probes for which the signal is inherently weak. The MRI method is schematically depicted in Figure 2.

During image acquisition, for encoding in the y direction, the magnetic resonance signal is given by

$$S(k_y) = \int \rho_o \exp\left[\frac{-n(\mathrm{TE})}{T_2}\right] \exp\left[i2\pi k_y y\right] dy \qquad (20)$$

where ρ_o is the nuclear spin density, $k_y = (2\pi)^{-1} \times \gamma G_y t_p$ (where G_y is the imaging gradient and t_p is the phase encoding time) is the space frequency, TE is the echo time, and n refers to the nth echo. The Fourier transform of eq. (20) yields an image

$$\rho(y) = \rho_o \exp\left[-\frac{n(\mathrm{TE})}{T_2(y)}\right] \qquad (21)$$

where $\rho(y)$ is the apparent nuclear spin density reduced from the true spin density by the T_2 decay.

The field of view (FOV) of the reconstructed image is given by

$$\mathrm{FOV} = \frac{1}{\Delta k_y} = \frac{1}{\frac{\gamma}{2\pi}\Delta G_y t_p} \qquad (22)$$

with a nominal image resolution of

$$\Delta y = \frac{\mathrm{FOV}}{N} \qquad (23)$$

where N is the number of k_y points acquired.

The measurements were performed in a Nalorac 8-cm, vertical-bore, 4.8-T (resonance frequency of 30.5 MHz for ^{2}H) magnet equipped with a self-shielded, water-cooled, magnetic field gradient set (DSI-873, Doty Scientific, Inc., Columbia, SC). The 90 and 180° pulse lengths were 46.5 and 93 μs, respectively, with a 60-W radio-frequency amplifier (M3205A, American Microwave Technology, Inc., Anaheim, CA). The nonuniform nature of the surface coil B_1 field necessitated an XY4 phase cycling scheme to minimize pulse length errors.[16,17] t_p and TE were 2 and 3.5 ms, respectively. A total of 12 echoes were acquired. During the acquisition, spoil gradients were used to avoid unwanted stimulated echoes.[18] The longitudinal magnetization recovery constant (T_1) of the sample varied between 50 and 80 ms during the course of the experiment. The delay between scans was set to 400 ms ($\geq 5T_1$), whereas the delay between gradient steps was 200 ms. This resulted in a reduced acquisition time with minimal T_1 blurring. A total of 64 k_y data points were acquired with 512 signal averages, which resulted in a signal-to-noise ratio of 36 for the image corresponding to an immersion time of 2.5 months. The total acquisition time for each profile was 2 h 20 min. During that period, the sample was wrapped in polytetrafluoroethylene tape to minimize the loss of D_2O due to evaporation. Weight measurements

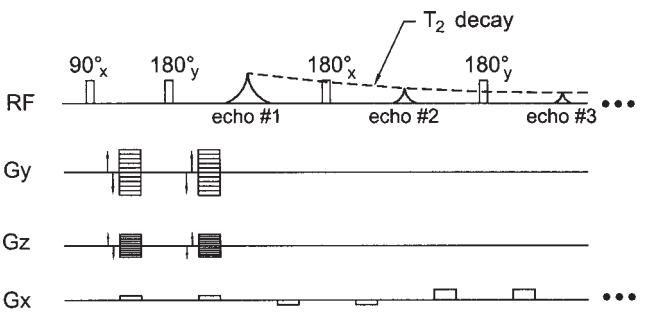

Figure 2 MRI pulse sequence for the spin-echo single-point imaging technique. RF represents the radio-frequency excitation and signal acquisition. The time between the 90° pulse and the first echo is the echo time (TE). G_y and G_z are the imaging gradients, and G_x is the spoil gradient. The total time of application of G_y (or G_z) is t_p.

showed that moisture loss during the acquisition was negligible. Similarly to Ouriadov et al.,[16] a linear combination of phase encoding gradients (G_y and G_z) was used to adjust the imaging direction so that it was perpendicular to the sample surface. Orientation around the z axis was carried out physically by the rotation of the probe inside the magnet.

RESULTS AND DISCUSSION

Sample moisture-absorption curve

The moisture-absorption curve for FM300 epoxy in D_2O at 70°C is shown in Figure 3. The figure also includes uptake curves obtained by fitting to Fickian and Langmuir models, the two most widely accepted models in the literature, and two models that have recently been shown to yield good results for moisture absorption by viscoelastic materials. The first viscoelastic model features a time-varying diffusion coefficient,[10] and the second model features a time-varying surface concentration.[9]

It can be seen from Figure 3 that diffusion does not follow a pure Fickian process except during the very early stages of absorption. The Fickian model predicts that saturation will be reached more rapidly than has been proven by experimentation. This anomaly has been observed and described by other investigators.[4] The Langmuir model and especially the time-varying diffusion model and time-varying surface concentration model follow the moisture-absorption trend more closely. However, model performance in describing moisture absorption does not guarantee an accurate moisture distribution. A comparison of moisture distributions from these models with experimental data is shown in a subsequent section.

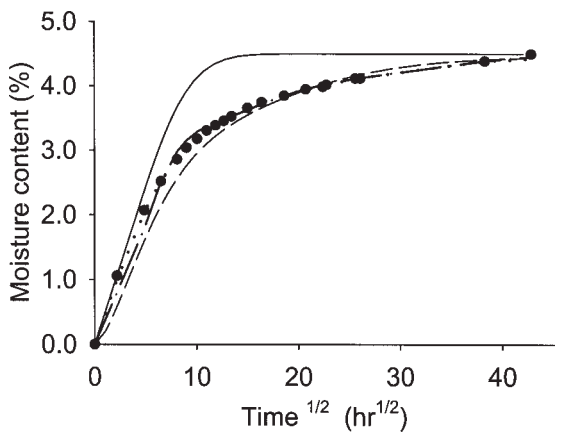

Figure 3 Moisture-uptake curve for D_2O in epoxy at 70°C. The moisture content is given by M (%) = (weight − $\text{weight}_{\text{dry}}$)/$\text{weight}_{\text{dry}}$ × 100. Curves are presented for (●) the weight-gain data, (—) Fickian model, (---) Langmuir model, (···) time-varying diffusivity model, and (-·-) time-varying boundary condition model.

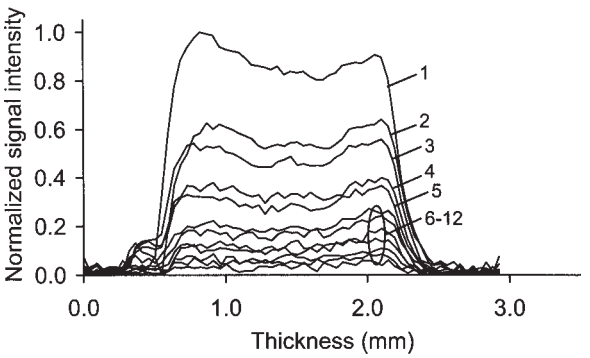

Figure 4 Multi-echo one-dimensional image of D_2O in epoxy. The echo time for the acquisition was 3.5 ms. The profiles shown correspond to an immersion time of 430 h. The numbers on the right are the echo numbers.

Moisture profiles

Each set of echoes collected from the multiple-spin-echo method, upon Fourier transformation, produced an image of the diffusion profile with decreasing intensity with the echo number (see Fig. 4). These sets of images were used to back-extrapolate the data to echo time 0 and obtain T_2-weighting free profiles[19] of free water in epoxy. The back-extrapolation was performed by fitting to eq. (21) with the IDL mpcurvefit least-squares fitting routine, which is based on the Marquardt–Levenberg algorithm. The resulting profiles are shown in Figure 5.

The moisture profiles of Figure 5 are quite revealing. It is clear that the exposed surfaces did not saturate immediately after first contact with water. In fact, the water content near the surface and across the sample increased continuously during the experi-

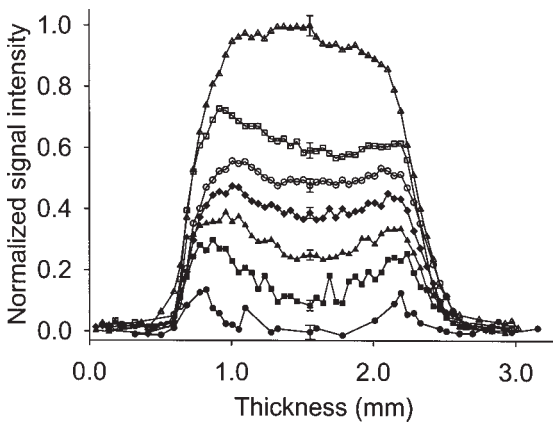

Figure 5 D_2O diffusion profiles in epoxy. The error bar at the center of each profile represents the typical standard error associated with the back-extrapolation operation. Profiles are presented for immersion times of (●) 42, (■) 81, (▲) 121, (◆) 181, (○) 269, (□) 430, and (△) 1830 h. A few erroneous data points (detected by visual inspection) were removed from the profile corresponding to 42 h of immersion.

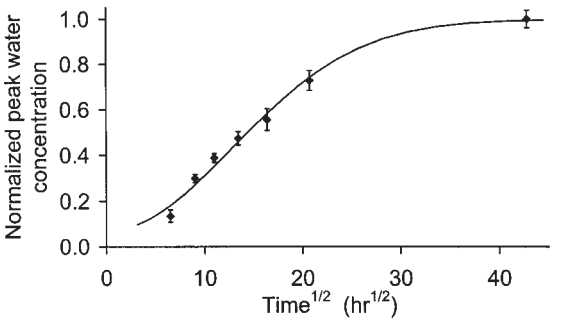

Figure 6 Evolution of the image intensity with the immersion time. The experimental data points are represented by diamonds. The solid line represents the best fit from an exponential rise to a maximum function.

ment. This suggests that there is a mechanism that increases the solubility of water (D_2O) in epoxy with time. Figure 6 presents a plot of the evolution of the peak (edge) moisture content with time. The local mobile water content at the edge appears to follow exponential growth. This is in agreement with Weitsman's assumption that viscoelastic relaxation phenomena cause a change in the surface concentrations with time.[6,9]

It is important to note that the profiles presented in Figure 5 are not pure D_2O density profiles but are rather mobile D_2O profiles. This is due to the existence of two components in the T_2 signal decay from D_2O in epoxy.[20] The short-lived signal is characteristic of bound D_2O, whereas the long-lived signal is associated with mobile D_2O. In our case, bulk Carr-Purcell-Meiboom-Gill (CPMG)[21] measurements with short (0.63 ms) and long (3.5 ms) echo times showed that the long component of the biexponential T_2 decay varied from 6 to 15 ms. Although a short component existed, it could not be determined on the basis of these measurements. The T_2 lifetime of bound D_2O was evaluated to be 300 μs by solid-state 2H-NMR.[22] With the echo time chosen to be 3.5 ms, the short component completely decayed in the imaging measurement. Therefore, the profiles reveal only the long component associated with the mobile D_2O.

Estimation of the amount of bound water

Despite the complete decay of the short-T_2, bound water in our imaging experiment, it is still possible to estimate the quantity of bound water present in the sample on the basis of the moisture-uptake data. Figure 7 presents a plot of the moisture content (obtained by weighing) against a normalized MRI signal intensity, which corresponds to the area under the profile curves of Figure 5. Figure 7 indicates that there is a linear relationship between the integrated MRI signal and the moisture content. A best fit line through the data points is also shown in Figure 7. It is interesting to note that this curve intercepts the moisture-content axis at $\sim$ 2.6%. This reveals the existence of a threshold value of moisture content below which no MRI signal is detected from the sample. Above 2.6% moisture content, any increase in the moisture content is detected in the MRI signal. We assume here that 2.6% corresponds to the amount of bound water in the epoxy sample. Furthermore, it means that 2.6% bond water is absorbed almost immediately throughout the sample. This represents over half (58%) of the total moisture uptake after 2.5 months of immersion and is absorbed in less than 40 h. Therefore, it is postulated that moisture must fill all the bonding sites first before diffusion can occur within the free volume of the epoxy network. In addition, except for the surface and because there is no reason *a priori* for the distribution of the bonding sites to be nonuniform, we can assume that the first step in the absorption process is one during which moisture is absorbed quickly by the polymer, resulting in a uniform distribution of bound water.

Moisture-absorption models

We now compare the experimental data to the four general classes of moisture-absorption models.

Fickian model

The Fickian absorption curve shown in Figure 3 is based on a saturation moisture content of 4.5%, which is the value of the water content after 2.5 months (1830 h) of immersion, and a diffusion coefficient calculated with eq. (6). The diffusion coefficient was evaluated to be 5.5×10^{-3} mm^2/h.

The values of the diffusivity and moisture content are based on weight-gain data exclusively and are now used in eq. (3) to predict moisture distribution profiles. The predicted Fickian moisture distributions

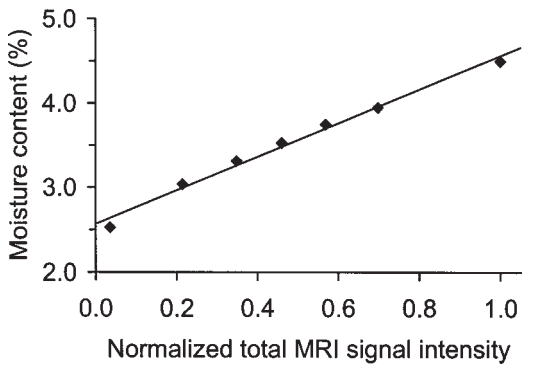

Figure 7 Moisture content plotted against the area under the profiles shown in Figure 4. The intercept ($\sim$ 2.6%) represents the amount of bound water. The diamonds represent the experimental data points. The solid line represents the best linear fit.

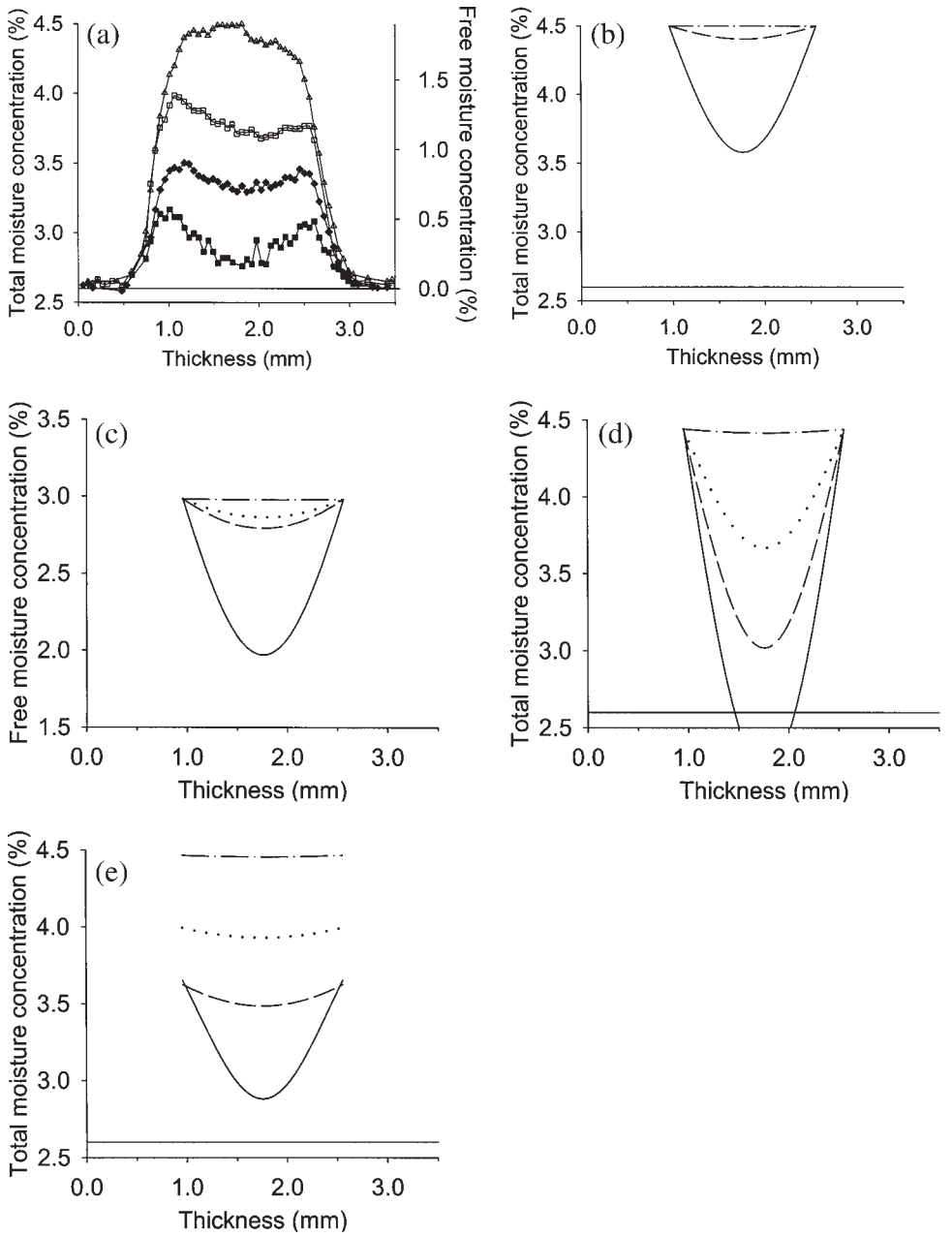

Figure 8 Moisture distribution profiles: (a) MRI measurement, (b) Fickian model, (c) Langmuir model, (d) time-varying diffusivity model, and (e) time-varying boundary condition model. (■,◆,□,△) MRI profiles and (—,---,···,-·-) model profiles are presented for immersion times of 81, 181, 430 and 1830 h, respectively.

at four different immersion times (81, 181, 430, and 1830 h) are presented in Figure 8(b). For evaluation, Figure 8(a) shows MRI moisture distributions at the corresponding times. For ease of comparison, all plots are presented in terms of the relative concentration by weight. The MRI profiles were offset by 2.6% to account for an assumed underlying uniform distribution of bound water. It is clear from Figure 8(a,b) that the Fickian model is inadequate to represent the moisture-absorption process in these samples. The main weakness of this model is its assumption that the surface concentration reaches saturation instantly, and this is not the case according to the MRI data.

Langmuir model

The Langmuir absorption curve (Fig. 3) was obtained by the fitting of eq. (19) to the weight-gain data with the least-squares method. The fitting was performed with a Sigmaplot® (Systat Software, Inc., San Jose, CA) using the Marquardt–Levenberg algorithm. The parameters extracted from the fit are $D = 4.3 \times 10^{-3}$ mm^2/h, $M_\infty = 4.45\%$, $\gamma = 1.21 \times 10^{-3}$, and $\beta = 2.46$

$\times 10^{-3}$. The values of γ and β indicate that at saturation ($\gamma c_{f\infty} = \beta c_{b\infty}$), the predicted ratio of the amount of bound water to total water is 0.33, which is lower than that deduced from the MRI data (0.58).

The moisture distribution predictions from the Langmuir model are presented in Figure 8(c). In this case, the free water concentration (rather than total water concentration) is plotted on the vertical axis. These moisture-concentration values should be compared with values from the right-hand side axis of Figure 8(a). The Langmuir model predicted a maximum free water concentration of 3.0 wt % across the sample after 1830 h of immersion, whereas a maximum concentration value of 1.9% was estimated from the MRI results. This difference is a direct result of the values of γ and β. Therefore, on the basis of the MRI data, the Langmuir model is in error for the estimation of the free water content. In addition, similarly to the Fickian model, the Langmuir model predicts an instantaneous moisture saturation of the exposed surfaces. The experimental data have shown that this is not the case. Nevertheless, the MRI data clearly indicate the presence of a bound water component.

Time-varying diffusivity model

The moisture-absorption curve (Fig. 3) from the time-varying diffusion coefficient model was obtained by the fitting of eq. (9) to the experimental data points with the least-squares method. The fitting was performed with the IDL mpcurvefit routine. A total of four terms were used in the Prony series, and the resulting parameters are as follows: M_∞ = 4.4%, D_0 = 0.00523 mm^2/h, $D_1 = -3.8 \times 10^{-3}$ mm^2/h, τ_1 = 39 h, $D_2 = -6.1 \times 10^{-3}$ mm^2/h, τ_2 = 391 h, $D_3 = 2.4 \times 10^{-3}$ mm^2/h, τ_3 = 412 h, $D_4 = 1.6 \times 10^{-3}$ mm^2/h, τ_4 = 520 h, $D_4 = 1.8 \times 10^{-3}$ mm^2/h, and τ_4 = 851 h.

The moisture distribution predictions from this model are presented in Figure 8(d). As for the two previous models, this model's main disadvantage is that it assumes that the saturation of the surfaces occurs instantly. Additionally, in this case, the time-varying diffusion coefficient slows down the diffusion of free water toward the center of the sample. This can be observed in a comparison of the curvature in the profiles with the corresponding profiles of the Fickian model [Fig. 8(a)]. As a result, the moisture distribution predictions lie further from the MRI data than the Fickian distribution. Therefore, this model is not recommended to model moisture absorption in this case.

Time-varying surface concentration model

The moisture-absorption curve (Fig. 3) from the time-varying surface concentration model was obtained by the fitting of eq. (14) to the weight-gain data. A total of five terms were used in the Prony series, and the resulting parameters are as follows: $D = 4.9 \times 10^{-3}$ mm^2/h, c_0 = 5.545, c_1 = 0.149, c_2 = −4.104, c_3 = 2.135, c_4 = −0.0554, c_5 = 0.946, β_1 = 1/10 h^{-1}, β_2 = 1/50 h^{-1}, β_3 = 1/100 h^{-1}, β_4 = 1/500 h^{-1}, and β_5 = 1/1000 h^{-1}.

The moisture distribution predictions from the time-varying surface concentration model are presented in Figure 8(e). Although not perfectly accurate, this model predicts the moisture absorption better than all previous models, especially for longer immersion times. The model yields reasonable values of surface concentrations and gives good predictions of the diffusion toward the center of the sample, as shown by the similarities in the curvatures between the predicted and MRI profiles. Of the four models investigated, this one is best suited to predict the absorption of water by epoxy under the experimental conditions.

CONCLUSIONS

A novel MRI technique, spin-echo single-point imaging, has been presented to measure the moisture distribution in an epoxy-adhesive polymer. This technique is very sensitive and therefore well suited to the study of diffusion in thin plates of adhesives. The technique was applied to study the absorption of moisture (D_2O) by a high-temperature aerospace-grade epoxy (FM300). Weight-gain data showed that this process was of the anomalous diffusion type.

The acquisition of data with the MRI technique employed was fast—2 h 20 min for the collection of T_2-weighted profiles—in comparison with the kinetics of moisture absorption, thus allowing for this time-resolved study. The MRI moisture profiles, which reflected the concentration of free water across the thickness of the sample plate, showed that the surface of the epoxy adhesive, a viscoelastic material, did not instantly saturate, contrary to the assumption employed in common diffusion model formulations. In fact, experimental data revealed that, after 2.5 months (1830 h) of immersion in D_2O at 70°C, the surface water concentration of the epoxy was still increasing. Although previous models were established on the basis of this concept, to the authors' knowledge, this is the first time that this phenomenon has been directly observed.

The MRI results, in conjunction with weight-gain data, allowed the estimation of the quantity of bound water in the epoxy, which was evaluated at 58% of the total moisture content after 2.5 months of immersion. The bound water was absorbed very early in the process: less than 40 h. The results of this MRI study suggest the existence of three distinct processes in the absorption of moisture by epoxy: the rapid absorption of bound water, the diffusion of free water, and the increase of the surface concentration. The latter could

be a reflection of viscoelastic relaxation, which increases solubility by increasing the free volumes.

Finally, the MRI moisture distribution profiles were used to evaluate the performance of the Fickian model as well as three additional models that were previously shown to describe anomalous diffusion in terms of total moisture uptake. The results showed that the model featuring time-varying boundary conditions best represents the anomalous moisture distribution in a fully crosslinked epoxy. The other models, that is, the Langmuir and time-varying diffusivity models, showed poorer predictions. It should be noted, however, that the study is phenomenological because the chemical structure of the epoxy system is unknown. It is possible that the time-varying boundary condition model applies only to this specific epoxy. Other epoxies will need to be evaluated to verify the general applicability of the model. In any case, this work has clearly demonstrated that diffusion models based only on moisture-uptake analysis should be used with caution.

One of the authors (G.L.) thanks the Natural Sciences and Engineering Research Council of Canada for a postgraduate scholarship B award. This author also thanks the Canadian Council for Professional Engineers and the Association of Professional Engineers and Geoscientists of New Brunswick for graduate scholarships. Two of the authors (G.L. and A.V.O.) thank Rod MacGregor for his assistance with the equipment. Two of the authors (P.L.-S. and B.J.B.) thank Captain Sylvain Giguère and Ken McRae for their expert advice. One of the authors (B.J.B.) thanks the Canada Chairs Program for a Research Chair in MRI of Materials.

References

1. Lee, M. C.; Peppas, N. A. Prog Polym Sci 1993, 18, 947.
2. LaPlante, G.; Lee-Sullivan, P. Proceedings of the Fourth Canadian–International Composites Conference, CANCOM 2003, Ottawa, Canada, Aug 19–22, 2003.
3. Giguère, J. S. R. Damage Mechanisms and Nondestructive Testing in the Case of Water Ingress in CF-18 Flight Control Surfaces, Tech. Rep. No. DCIEM TM 2000–098, Defense and Civil Institute of Environmental Medicine, Canada (August 2000).
4. Weitsman, Y. J. In Comprehensive Composite Materials; Talreja, R.; Manson, J.-A. E., Eds.; Elsevier: Amsterdam, 2000; Vol. 2.
5. Apicella, A.; Nicolais, N. Advances in Polymer Science; Dusek, K., Ed., Springer-Verlag: Berlin, 1986; Vol. 72, p 69.
6. Weitsman, Y. In Fatigue of Composite Materials; Reifsnider, K. L., Ed.; Elsevier: Amsterdam, 1990; Chapter 9.
7. Crank, J. The Mathematics of Diffusion; Oxford University Press: Oxford, 1975.
8. Carter, H. G.; Kibler, K. G. J Compos Mater 1978, 12, 118.
9. Cai, L.-W.; Weitsman, Y. J Compos Mater 1994, 28, 130.
10. Roy, S.; Xu, W. X.; Park, S. J.; Liechti, K. M. J Appl Mech 2000, 67, 391.
11. Maggana, C.; Pissis, P. J Polym Sci Part B: Polym Phys 1999, 37, 1165.
12. Koenig, J. L. Microspectroscopic Imaging of Polymers; American Chemical Society: Washington, DC, 1998.
13. Shen, C.-H.; Springer, G. S. J Compos Mater 1976, 10, 2.
14. ASTM D 5229-M–92. Annu Book ASTM Stand; American Society for Testing and Materials: West Conshohocken, PA, 1995, Vol. 15.03, p 216.
15. Spatially Resolved Magnetic Resonance; Blümer, P.; Blümich, B.; Botto, R.; Fukushima, E., Eds.; Wiley-VCH: Weinheim, 1998.
16. Ouriadov, A. V.; MacGregor, R. P.; Balcom, B. J. J Magn Res 2004, 169, 174.
17. Maudsley, A. A. J Magn Res 1986, 69, 488.
18. Crawley, A. P.; Henkelman, R. M. Magn Res Med 1987, 4, 34.
19. Cano Barrita, F. J.; Bremner, T. W.; Balcom, B. J.; MacMillan, M. B.; Langley, W. S. Mater Struct 2004, 37, 522.
20. Klotz, J.; Brostow, W.; Hess, M.; Veeman, W. S. Polym Eng Sci 1996, 36, 1129.
21. Meiboom, S.; Gill, D. Rev Sci Instrum 1958, 29, 688.
22. Kintanar, A.; Huang, W.-C.; Schindele, D. C.; Wemmer, D. E.; Drobny, G. Biochemistry 1989, 28, 282.